

Atomic carbon at redshift ~ 2.5

A. Weiß¹, D. Downes², C. Henkel³, and F. Walter⁴

¹ IRAM, Avenida Divina Pastora 7, 18012 Granada, Spain

² IRAM, 300 rue de la Piscine, 38406 St-Martin-d'Hères, France

³ MPIFR, Auf dem Hügel 69, 53121 Bonn, Germany

⁴ MPIA, Königstuhl 17, 69117 Heidelberg, Germany

Abstract. Using the IRAM 30m telescope we detected the lower fine structure line of neutral carbon ($\text{C I}(^3P_1 \rightarrow ^3P_0)$, $\nu_{\text{rest}} = 492$ GHz) towards three high-redshift sources: IRAS FSC 10214 ($z = 2.3$), SMM J14011+0252 ($z = 2.5$) and H1413+117 (Cloverleaf quasar, $z = 2.5$). SMM J14011+0252 is the first high-redshift, non-AGN source in which C I has been detected. The $\text{C I}(^3P_1 \rightarrow ^3P_0)$ line from FSC 10214 is almost an order of magnitude weaker than previously claimed, while our detection in the Cloverleaf is in good agreement with earlier observations. The $\text{C I}(^3P_1 \rightarrow ^3P_0)$ linewidths are similar to the CO widths, indicating that both lines trace similar regions of molecular gas on galactic scales. Derived $\text{C I}(^3P_1 \rightarrow ^3P_0)$ masses for all three objects are of order few $\times 10^7 M_{\odot}$ and the implied $\text{C I}(^3P_1 \rightarrow ^3P_0)/^{12}\text{CO}(J=3 \rightarrow 2)$ line luminosity ratio is about 0.2. This number is similar to values found in local galaxies. We derive a C I abundance of 5×10^{-5} which implies significant metal enrichment of the cold molecular gas at redshifts 2.5 (age of the universe 2.7 Gyr). We conclude that the physical properties of systems at large lookback times are similar to today's starburst/AGN environments.

Key words. galaxies: formation – galaxies: high-redshift – galaxies: ISM – galaxies: individual (SMM J14011+0252) – quasars: individual (Cloverleaf, IRAS F10214+4724) – cosmology: observations

1. Introduction

Investigating the dense cool interstellar medium in high redshift galaxies is of fundamental importance for our understanding of the early phases of galaxy formation and evolution. Recent studies have revealed the presence of huge molecular gas quantities ($> 10^{10} M_{\odot}$) in distant objects, which show that the gas reservoirs for powerful starbursts are present in the early universe (for a review see Carilli et al. 2004). So far, molecular gas has been detected in about 25 sources at $z > 2$, out to a redshift of $z = 6.4$ (Walter et al. 2003, Bertoldi et al. 2003).

The brightest and therefore most common tracer for molecular gas is carbon monoxide (CO). Multi-transition studies of CO lines can be used to constrain the physical properties of the molecular gas. However, the interpretation of optically thick CO lines is not straightforward and requires detailed modeling (e.g., radiative transfer codes). To constrain these models, observations of faint optically thin lines (such as e.g., ^{13}CO) are needed (e.g. Weiß et al. 2001) which are, however, inaccessible given current limitations in sensitivity.

Observations of neutral carbon (C I) can help to circumvent these problems. Because the 3P fine-structure system of carbon forms a simple three-level system, detections of *both* optically thin carbon lines, $\text{C I}(^3P_1 \rightarrow ^3P_0)$ (492 GHz) and $\text{C I}(^3P_2 \rightarrow ^3P_1)$ (809 GHz), in principle allow us to de-

rive the excitation temperature, neutral carbon column density and mass independently of any other information (e.g. Stutzki et al. 1997, Weiß et al. 2003).

Although the atmospheric transmission is poor at the C I rest frequencies, a number of studies of neutral carbon have been carried out in molecular clouds of the galactic disk, the galactic center, M82 and other nearby galaxies (e.g., White et al. 1994; Stutzki et al. 1997; Gerin & Phillips 2000; Ojha et al. 2001; Israel & Baas 2002; Schneider et al. 2003, Kramer et al. 2004). These studies have shown that C I is closely associated with the CO emission independent of the environment. Since the critical density for the $\text{C I}(^3P_1 \rightarrow ^3P_0)$ and $^{12}\text{CO}(J=1 \rightarrow 0)$ lines are both $n_{\text{cr}} \approx 10^3 \text{ cm}^{-3}$ this finding suggests that the transitions arise from the same volume and share similar excitation temperatures (e.g. Ikeda et al. 2002).

In this letter we report on the detection of the lower fine structure line of atomic carbon, $\text{C I}(^3P_1 \rightarrow ^3P_0)$, towards the three strongest molecular line emitters at redshifts > 2 currently known: IRAS FSC 10214 ($z = 2.29$, F10214 thereafter), SMM J14011+0252 ($z = 2.57$, SMM14011 thereafter) and H1413+117 (Cloverleaf Quasar, $z = 2.56$). We use a Λ cosmology with $H_0 = 71 \text{ km s}^{-1} \text{ Mpc}^{-1}$, $\Omega_{\Lambda} = 0.73$ and $\Omega_m = 0.27$ (Spergel et al. 2003).

2. Observations

Observations were carried out with the IRAM 30 m telescope from Sep. 2003 to July 2004. We used the CD receiver configuration with the C/D 150 receivers tuned to the $\text{C I}(^3P_1 \rightarrow ^3P_0)$ transition. For each source the observing frequency of the $\text{C I}(^3P_1 \rightarrow ^3P_0)$ transition is listed in Table 1. The beam size at 140 GHz is $\approx 17''$. Typical system temperatures were ≈ 200 K and ≈ 270 K (T_A^*) during winter and summer respectively. The observations were carried out in the wobbler switching mode, with a switching frequency of 0.5 Hz and a wobbler throw of $50''$ in azimuth. Pointing was checked frequently and was found to be stable within $3''$. Calibration was obtained every 12 min using the standard hot/cold-load absorber measurements. The planet Mars was used for absolute flux calibration. The antenna gain was found to be consistent with the standard value of 6.6 Jy/K at 140 GHz. We estimate the flux density scale to be accurate to about $\pm 15\%$. Data were recorded using the 4 MHz filter banks on each receiver (512 channels, 1 GHz bandwidth, 4 MHz channel spacing). The data were processed using the CLASS software. After dropping bad data only linear baselines were subtracted from individual spectra. The resulting profiles were regridded to a velocity resolution of 55 km s^{-1} (F10214), 65 km s^{-1} (SMM14011) and 70 km s^{-1} (Cloverleaf) leading to an RMS of 0.25 mK (1.7 mJy), 0.24 mK (1.6 mJy) and 0.25 mK (1.7 mJy), respectively. The on-source integration time in the final spectra is 8h, 10.5h and 4.5h for F10214, SMM14011 and the Cloverleaf respectively. The final spectra are presented in Fig. 1.

3. Results

3.1. F10214

Our new $\text{C I}(^3P_1 \rightarrow ^3P_0)$ spectrum towards F10214 does not confirm the $\text{C I}(^3P_1 \rightarrow ^3P_0)$ detection reported by Brown & Vanden Bout (1992, see Fig. 1 and Table 1 versus their Fig. 3). The integrated line flux is 7 times lower and the peak line antenna temperature of 1.4 mK is well within the noise level of the old observations. Given the superior quality of our new measurements, we consider the data presented here to be the first detection of C I in this object. The $\text{C I}(^3P_1 \rightarrow ^3P_0)$ redshift in F10214 is in agreement with the CO redshift but the carbon line is narrower. We attribute this to the limited signal to noise (≈ 6) in our observations. Our derived line parameters are summarized in Tab. 1. For F10214 we find a line luminosity (see e.g. Solomon et al. 1997 for a definition) ratio compared to $^{12}\text{CO}(J=3\rightarrow 2)$ of $L'_{\text{C I}(^3P_1 \rightarrow ^3P_0)}/L'_{^{12}\text{CO}(J=3\rightarrow 2)} = 0.19 \pm 0.05$ (see footnote of Table 1 for $^{12}\text{CO}(J=3\rightarrow 2)$ luminosities and references).

3.2. SMM14011

Our $\text{C I}(^3P_1 \rightarrow ^3P_0)$ detection in SMM14011 is the first atomic carbon detection reported in any high- z Scuba sub-mm galaxy. The absence of AGN characteristics in optical spectra (Barger et al. 1999, Ivison et al. 2000) together with the non detection of hard X-rays (Fabian et al. 2000) implies that the gas is mainly heated by star formation. The carbon line linewidth is slightly higher than the CO width and the spectrum shows a small velocity offset compared to the CO redshift – this is most likely due to the current limited signal to noise ratio. The C I to $^{12}\text{CO}(J=3\rightarrow 2)$ line luminosity ratio in SMM14011 is $L'_{\text{C I}(^3P_1 \rightarrow ^3P_0)}/L'_{^{12}\text{CO}(J=3\rightarrow 2)} = 0.32 \pm 0.06$.

3.3. The Cloverleaf

The Cloverleaf is a Broad-Absorption Line (BAL) quasar (QSO) with very broad high-excitation emission lines and is the brightest and best-studied high- z CO source. The redshift of the carbon line agrees with the CO redshift and the $\text{C I}(^3P_1 \rightarrow ^3P_0)$ linewidth of 360 km s^{-1} is similar to CO measurements (e.g. Weiß et al. 2003) and the previous neutral carbon detection by Barvainis et al. (1997). The integrated $\text{C I}(^3P_1 \rightarrow ^3P_0)$ flux density is in good agreement with the value reported by Barvainis. With our new $\text{C I}(^3P_1 \rightarrow ^3P_0)$ flux of $I_{\text{C I}} = 3.9 \pm 0.6 \text{ Jy km s}^{-1}$ we find a line luminosity ratio of $L'_{\text{C I}(^3P_1 \rightarrow ^3P_0)}/L'_{^{12}\text{CO}(J=3\rightarrow 2)} = 0.15 \pm 0.02$. Our observations confirm the low carbon fine structure line ratio of $L'_{\text{C I}(^3P_2 \rightarrow ^3P_1)}/L'_{\text{C I}(^3P_1 \rightarrow ^3P_0)} \approx 0.5$ (Weiß et al. 2003).

4. Discussion

4.1. $\text{C I}/\text{CO}$ line ratios and cooling

Judging from our $L'_{\text{C I}}/L'_{\text{CO}(3\rightarrow 2)}$ line luminosity ratios the carbon chemistry and/or excitation does not change strongly between a pure starburst (SMM14011) and the starburst/AGN (Cloverleaf, F10214) heated environment at redshifts ≈ 2.5 . For SMM14011 we find a slightly higher $L'_{\text{C I}}/L'_{\text{CO}(3\rightarrow 2)}$ line luminosity ratio than for the two QSOs. For local galaxies Gerin & Phillips (2000) find an average brightness temperature ratio between $\text{C I}(^3P_1 \rightarrow ^3P_0)$ and $^{12}\text{CO}(J=1\rightarrow 0)$ of 0.2 ± 0.2 independent of the environment. A similar ratio has also been found in Arp 220 (Gerin & Phillips 1998). Detailed radiative transfer models show that the $^{12}\text{CO}(J=1\rightarrow 0)$ and $^{12}\text{CO}(J=3\rightarrow 2)$ transitions are near thermal equilibrium ($L'_{\text{CO}(1\rightarrow 0)} \approx L'_{\text{CO}(3\rightarrow 2)}$) for all three sources studied here (Weiß et al. in prep.). This implies that the $\text{C I}(^3P_1 \rightarrow ^3P_0)/^{12}\text{CO}(J=1\rightarrow 0)$ ratio for dusty quasars and submm galaxies at $z \approx 2.5$ resembles those for local galaxies. The cooling via C I and CO for all three sources is small compared to the cooling due to thermal dust emission ($L_{\text{CO}}/L_{\text{FIR}} \leq 10^{-4}$) with CO being the more effective cooler compared to C I ($L_{\text{C I}}/L_{\text{CO}} \approx 0.05 - 0.2$).

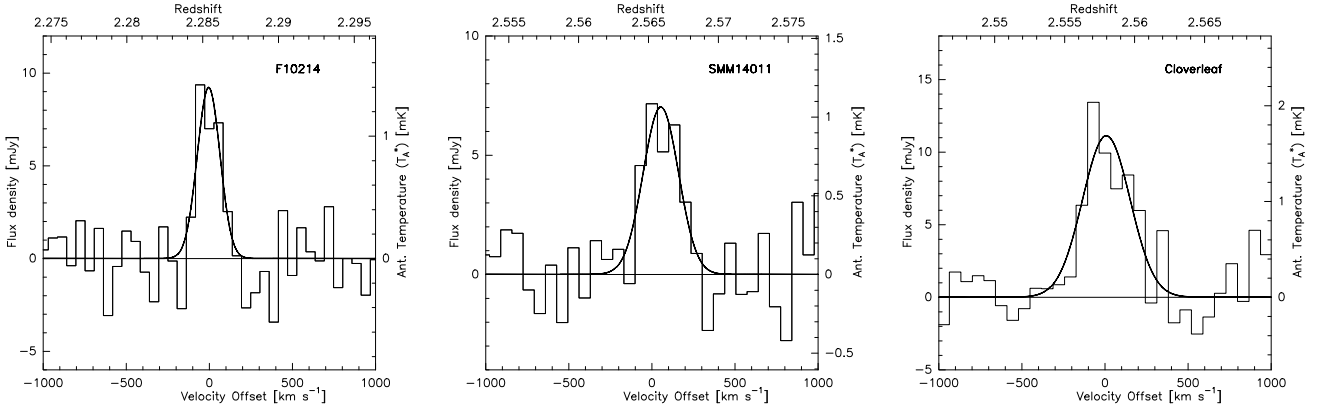


Fig. 1. Spectra of the $\text{C I}(^3P_1 \rightarrow ^3P_0)$ fine structure line towards F10214, SMM14011 and the Cloverleaf superposed on their Gaussian fit profiles (see Table 1 for parameters). The velocity scale is relative to the CO redshift given in the footnote of Table 1. The velocity resolution is 55 km s^{-1} (F10214), 65 km s^{-1} (SMM14011) and 70 km s^{-1} (Cloverleaf).

Table 1. Observed $\text{C I}(^3P_1 \rightarrow ^3P_0)$ line parameters.

Source	ν_{obs} [GHz]	T_A^* [mK]	S_ν [mJy]	ΔV_{FWHM} [km s^{-1}]	I [Jy km s^{-1}]	V_0 [km s^{-1}]	$L'_{\text{CI}}/10^{10}$ [K $\text{km s}^{-1} \text{ pc}^2$]	${}^d L'_{\text{CI}}/L'_{\text{CO}(3-2)}$
F10214	149.8024	1.4 ± 0.15	9.2 ± 1.0	160 ± 30	1.6 ± 0.2	^a -5 ± 12	2.2 ± 0.3	0.19 ± 0.05
SMM14011	138.0457	1.1 ± 0.2	7.3 ± 1.5	235 ± 45	1.8 ± 0.3	^b 45 ± 27	3.1 ± 0.5	0.32 ± 0.06
Cloverleaf	138.3313	1.8 ± 0.3	11.2 ± 2.0	360 ± 60	3.9 ± 0.6	^c 7 ± 25	6.7 ± 1.0	0.15 ± 0.02

Quoted errors are statistical errors from Gaussian fits. Systematic calibration uncertainty is $\pm 15\%$

^a Center velocity relative to $z=2.2854$ (Downes et al. 1995).

^b Center velocity relative to $z=2.5653$ (Frayer et al. 1999).

^c Center velocity relative to $z=2.5578$ (Weiß et al. 2003).

^d $L'_{\text{CO}(3-2)}$: F10214: $11.7 \pm 0.6 \times 10^{10} \text{ K km s}^{-1} \text{ pc}^2$ Solomon et al. (1992); SMM14011: $9.7 \pm 1.0 \times 10^{10} \text{ K km s}^{-1} \text{ pc}^2$ Downes & Solomon (2003); Cloverleaf $45.7 \pm 0.7 \times 10^{10} \text{ K km s}^{-1} \text{ pc}^2$ Weiß et al. (2003)

4.2. Neutral carbon mass and abundance

In analogy to the formulas given in Weiß et al. (2003) for the upper fine structure line of atomic carbon, $\text{C I}(^3P_2 \rightarrow ^3P_1)$, we can derive the total mass of neutral carbon using the luminosity of the lower fine structure line, $\text{C I}(^3P_1 \rightarrow ^3P_0)$, via

$$M_{\text{CI}} = C m_{\text{CI}} \frac{8\pi k \nu_0^2}{hc^3 A_{10}} Q(T_{\text{ex}}) \frac{1}{3} e^{T_1/T_{\text{ex}}} L'_{\text{CI}(^3P_1 \rightarrow ^3P_0)} \quad (1)$$

where $Q(T_{\text{ex}}) = 1 + 3e^{-T_1/T_{\text{ex}}} + 5e^{-T_2/T_{\text{ex}}}$ is the C I partition function. $T_1 = 23.6 \text{ K}$ and $T_2 = 62.5 \text{ K}$ are the energies above the ground state. m_{CI} is the mass of a single carbon atom and C is the conversion between pc^2 and cm^2 . The above equation assumes optically thin C I emission and that both carbon lines are in local thermodynamical equilibrium (LTE). Inserting numbers yields: ¹

$$M_{\text{CI}} = 5.706 \times 10^{-4} Q(T_{\text{ex}}) \frac{1}{3} e^{23.6/T_{\text{ex}}} L'_{\text{CI}(^3P_1 \rightarrow ^3P_0)} [\text{M}_\odot] \quad (2)$$

¹ In our previous paper (Weiß et al. 2003) the similar equation for the carbon mass derived from the upper fine structure line (Eq. 3) should have a coefficient of 4.556×10^{-4} . All the carbon masses quoted in the text, however, are correct.

The determination of the excitation temperature of atomic carbon requires the measurement of both fine structure lines. The upper carbon fine structure line so far has only been detected in the Cloverleaf Quasar (Weiß et al. 2003) yielding $T_{\text{ex}} = 30 \text{ K}$ ($T_{\text{dust}} = 50 \text{ K}$). As the excitation temperature is a priori unknown for the other two sources we here assume $T_{\text{ex}} = 30 \text{ K}$ as derived for the Cloverleaf. Similar excitation temperatures for all three sources are motivated by similar dust temperatures (F10214: $T_{\text{dust}} = 55 \text{ K}$ Benford et al. 1999; SMM14011: $T_{\text{dust}} = 50 \text{ K}$ Ivison et al. 2000). We note however that the total neutral carbon mass is not a strong function of the assumed T_{ex} unless the excitation temperature is below 20 K (see Fig. 2). The resulting carbon masses (uncorrected for the magnification m) are listed in Table 2. Table 2 also lists the H_2 masses derived from the $^{12}\text{CO}(J=3 \rightarrow 2)$ line luminosity. Here we assume a ULIRG conversion factor of $M_{\text{H}_2}/L'_{\text{CO}} = 0.8 \text{ M}_\odot (\text{K km s}^{-1} \text{ pc}^2)^{-1}$ (Downes & Solomon 1998). The mass ratio between C I and H_2 allows us to estimate the neutral carbon abundance relative to H_2 via $X[\text{C I}]/X[\text{H}_2] = M(\text{C I})/(6 M(\text{H}_2))$. Note that the carbon abundance is independent of the magnification (disregarding differential magnification) and the applied

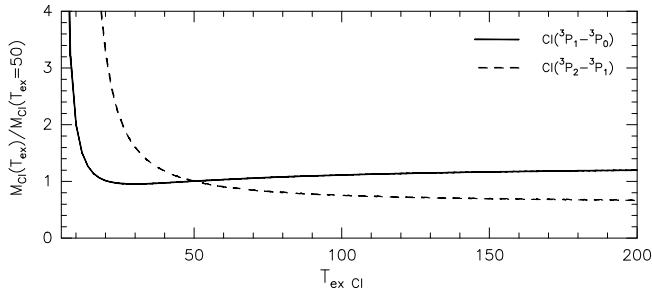


Fig. 2. Dependence of the neutral carbon mass on the carbon excitation temperature assuming LTE. The carbon mass is normalized to $T_{ex\text{ CI}} = 50$ K. The solid line corresponds to masses derived from the $\text{C I}(^3\text{P}_1 \rightarrow ^3\text{P}_0)$ line luminosity (Eq. 2), the dashed line is the corresponding plot of the $\text{C I}(^3\text{P}_2 \rightarrow ^3\text{P}_1)$ line luminosity.

Table 2. Mass and abundance of neutral carbon.

	F10214	SMM14011	Cloverleaf
$M_{\text{CI}} [M_{\odot}/10^7]$	$2.7 m^{-1}$	$3.9 m^{-1}$	$8.4 m^{-1}$
$M_{\text{H}_2} [M_{\odot}/10^{10}]$	$9.4 m^{-1}$	$7.8 m^{-1}$	$36.5 m^{-1}$
$X[\text{CI}]/X[\text{H}_2]$	4.9×10^{-5}	8.3×10^{-5}	3.8×10^{-5}

m denotes the magnification due to gravitational lensing

cosmology. We find a carbon abundance of $X[\text{CI}]/X[\text{H}_2] \approx 5 \times 10^{-5}$ for all sources. This value is similar to the C I abundance in the Galaxy of $X[\text{CI}]/X[\text{H}_2] = 2.2 \times 10^{-5}$ (Frerking et al. 1989). This implies that the cold molecular gas in these systems at redshift 2.5 is already substantially enriched. This finding is in line with abundance determinations for high redshift QSOs using optical spectra (e.g. Dietrich et al. 2003) albeit for the cold molecular gas phase. For local starburst galaxies it has been found that the neutral carbon gas phase abundance tends to be higher than in the Milky Way (e.g. Schilke et al. 1993, White et al. 1994, Israel & Baas 2001, 2003). However, given the underlying assumptions of H_2 mass determinations in high- z sources, our data do not allow us to investigate possible C I abundance variations between QSO and starburst heated environments in more detail.

We conclude that the physical properties of systems at large lookback times ($z = 2.5$ corresponds to an age of the universe of only 2.7 Gyr) are similar to today's starburst/AGN environments. Our study also shows that C I is one of the brightest tracers of the cold molecular gas in galaxies. It therefore provides a powerful diagnostic of galaxy evolution well beyond $z = 2.5$, especially in the light of the next generation of mm and sub-mm telescopes (such as ALMA).

Acknowledgements. IRAM is supported by INSU/CNRS (France), MPG (Germany) and IGN (Spain).

References

- Barger, A.J., Cowie, L.L., Smail, I., Ivison, R.J., Blain, A.W., & Kneib, J.P. 1999, *AJ*, 117, 2656
- Barvainis, R., Maloney, P., Antonucci, R., & Alloin, D. 1997, *ApJ*, 484, 695
- Benford, D.J., Cox, P., Omont, A., Phillips, T.G., & McMahon, R.G. 1999, *ApJ*, 518, L65
- Bertoldi, F., Cox, P., Neri, R., et al. 2003, *A&A*, 409, L47
- Brown, R.L., & Vanden Bout, P.A. 1992, *ApJ*, 397, L11
- Carilli, C.L., Bertoldi, F., Walter, F., Menten, K.M., Beelen, A., Cox, P., & Omont, A. 2004, *Multiwavelength AGN Surveys*, eds. Maiolino and Mujica (World Scientific)
- Dietrich, M., Hamann, F., Appenzeller, I., & Vestergaard, M. 2003, *ApJ*, 596, 817
- Downes, D., Solomon, P.M., & Radford, S.J.E. 1995, *ApJ*, 453, L65
- Downes, D., & Solomon, P.M. 1998, *ApJ*, 507, 615
- Downes, D., & Solomon, P.M. 2003, *ApJ*, 528, 37
- Fabian, A.C., Smail, I., Iwasawa, K., et al. 2000, *MNRAS*, 315, L8
- Frayer, D.T., Ivison, R., Scoville, N.Z., et al. 1999, *ApJ*, 514, L13
- Frerking, M.A., Keene, J., Blake, G.A., & Phillips, T.G. 1989, *ApJ*, 344, 311
- Gerin, M., & Phillips, T.G. 1998, *ApJ*, 509, L17
- Gerin, M., & Phillips, T.G. 2000, *ApJ*, 537, 644
- Ikeda, M., Oka, T., Tatematsu, K., Sekimoto, Y., & Yamamoto, S. 2002, *ApJS*, 139, 467
- Israel, F.P., & Baas, F. 2001, *A&A*, 371, 433
- Israel, F.P., & Baas, F. 2002, *A&A*, 383, 82
- Israel, F.P., & Baas, F. 2003, *A&A*, 404, 495
- Ivison, R.J., Smail, I., Barger, A.J., Kneib, J.P., Blain, A.W., Owen, F.N., Kerr, T.H., & Cowie, L.L. 2000, *MNRAS*, 315, 209
- Kramer, C., Jakob, H., Mookerjee, B., Schneider, N., Bruell, M., & Stutzki, J. 2004, *A&A*, 424, 887
- Ojha, R., Stark, A.A., Hsieh, H.H., et al. 2001, *ApJ*, 548, 253
- Schneider, N., Simon, R., Kramer, C., Kraemer, K., Stutzki, J., & Mookerjee, B. 2003, *A&A*, 406, 915
- Schilke, P., Carlstrom, J.E., Keene, J., & Phillips, T.G. 1993, *ApJ*, 417, L67
- Solomon, P.M., Downes, D., & Radford, S.J.E. 1992, *ApJ*, 398, L29
- Solomon, P.M., Downes, D., Radford, S.J.E., & Barrett, W.J. 1997, *ApJ*, 478, 144
- Spergel, D.N., Verde, L., Peiris, H., et al. 2003, *ApJS*, 148, 175
- Stutzki, J., Graf, U.U., Haas, S., et al. 1997, *ApJ*, 477, L33
- Venturini, S., & Solomon, P.M. 2003, *ApJ*, 590, 740
- Walter, F., Bertoldi, F., Carilli, C.L., et al. 2003, *Nature*, 424, 406
- Weiß, A., Neinger, N., Hüttemeister, S., & Klein, U. 2001, *A&A*, 365, 571
- Weiß, A., Henkel, C., Downes, D., & Walter, F. 2003, *A&A*, 409, L41
- White, G.J., Ellison, B., Claude, S., Dent, W.R.F., & Matheson, D.N. 1994, *A&A*, 284, L23